33RD CONGRESS
OF THE INTERNATIONAL COUNCIL
OF THE AERONAUTICAL SCIENCES
STOCKHOLM, SWEDEN, 4-9 SEPTEMBER, 2022

ICAS 2022 SWEDEN

AEROELASTIC TAILORING OF COMPRESSOR BLADES

Akshay Prafulla Chalke[1], Nenad Glodic[1] & Mauricio Gutierrez Salas[1]

[1]KTH Royal Institute of Technology

Abstract

Paper explores the potential of using carbon-fibre reinforced composites for designing low-pressure compressor blades with improved aeroelastic performance. Comparison between the blades with different laminate stackups is made with respect to the modal behaviour and aerodynamic damping. It is found that if carefully designed, the composite blades can provide higher aeroelastic stability than the reference metallic blade.At the same time the results reveal that a laminate stackup with stabilizing behaviour in one mode could have a destabilizing effect for the other mode. The dependency on ply angle and arrangement of plies in laminates is observed to be complex and further investigations and experimental validation is therefore deemed necessary.

Keywords: composite blades, blade vibration, aerodynamic damping, tailoring

1. Introduction

The quest to achieve lighter and more efficient turbomachines has resulted in a drive to look for alternate materials and investigations into aeromechanical limitations. Carbon fiber composite has emerged as an alternative due to its light weight and anisotropic properties. The anisotropic nature has fueled the curiosity to investigate if it can be used to enhance mechanical performance and provide aeroelastic stability where traditional metallic blades would fall short of requirements. A tendency toward thinner, lighter and highly loaded blades in modern aircraft engine design gives rise to an increased sensibility for flow-induced vibration such as flutter. The flutter stability depends on the blade vibration in the flow field and the unsteady aerodynamic forces resulting from the vibrations. The induced unsteady aerodynamic forces are depending both on the flow conditions surrounding the blade and the blade motion. Since the aerodynamics are set by the design operating condition,the way to influence the aeroelastic behavior would be to alter the vibrational mode shape of the blade. The direction dependent stiffness in the carbon fiber composites offers the possibility to change the blade mode shape by adjusting the laminate layup without affecting the actual geometry of the blade [1],[2].

2. Test case and Composite Numerical model

The aim of the present investigation is to assess the effects of different laminate stacking in the carbon fibre reinforced composites on the aeroelastic (flutter) stability of a modern low-pressure compressor rotor blade.The study was carried out within the NFFP7 project called VIND (Virtual Integrated Demonstrator for turbomachinery), which is a collaborative project between GKN Aerospace Sweden AB, Chalmers, Lund and KTH. The analyzed test object is a front stage rotor of a modern 3-stage high-speed booster designed within the frame of the project[3] and represented in Figure 1

A composite blade model is built in Ansys Composite PrepPost (ACP) following composite design guidelines prescribed in literature [4], [5]. Materials pre-defined in Ansys library are used for analysis where Epoxy carbon UD(230 GPa) Prepreg is used as fabric and epoxy is used as the resin material. The ply thickness is set as 0.125 mm [4]. A camber surface with face mesh is used for generating

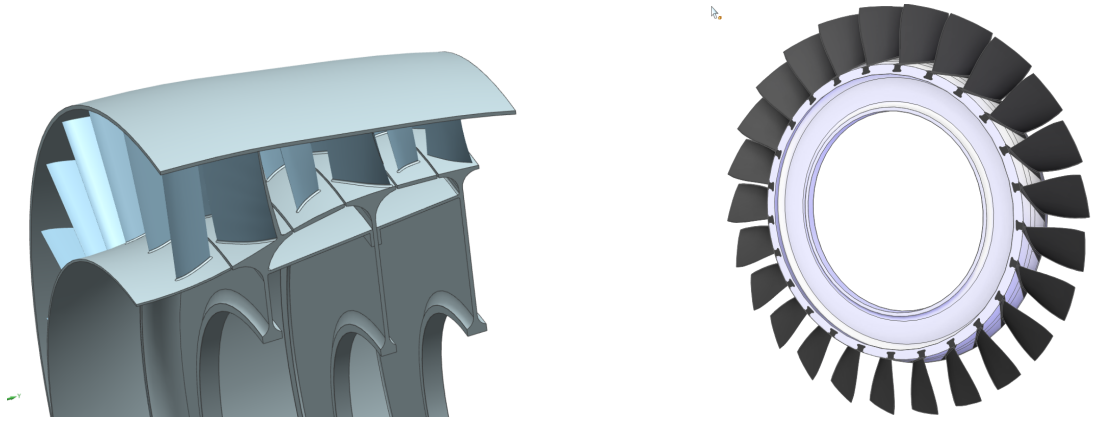

(a) VIND 3-stage high speed booster

(b) Front stage bladed disk with CF blades

Figure 1 – Test case

the solid composite model mesh (186918 Nodes). The plies are cut at various lengths so as to adjust to the blade shape and later shuffled to comply with the ply layup and ply drop criteria suggested in literature [4], [5]. A representation of the chord-wise lengths of each ply and the unshuffled and shuffled sequence is shown in Figure 2a and 2b where 1 is the outermost ply representing the suction or pressure surface and 25 is on the camber surface which represents the symmetry surface of the laminate. The plies are approximately centered on the mid chord as in Figure 2c. The reference 0° fabric direction is oriented along the span of the blade with axis towards the tip and positive ply angles defined in the clockwise sense when looking towards the suction side. Focus of the current investigation is on the blade only i.e. no dovetail is considered in the model.

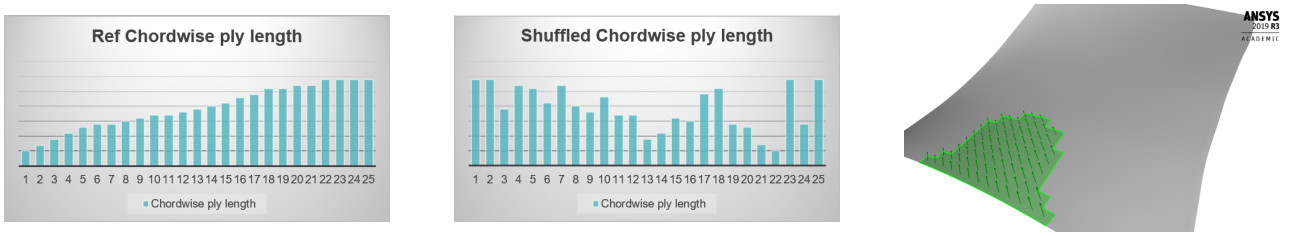

(a) Unshuffled ply stackup

(b) Shuffled ply stackup

(c) Representative ply

Figure 2 – Ply shuffling to comply design rules

Six different ply stackup configurations were investigated in the scope of project with a combination of ±60°, ±45°, ±22.5° and 0° plies. The investigated laminate stackups are shown in Table 1.

	Ply no																								
Stackup	**1**	**2**	**3**	**4**	**5**	**6**	**7**	**8**	**9**	**10**	**11**	**12**	**13**	**14**	**15**	**16**	**17**	**18**	**19**	**20**	**21**	**22**	**23**	**24**	**25**
1	60	45	22.5	0	-22.5	-45	-60	-45	-22.5	0	22.5	45	0	0	-60	-22.5	0	0	0	0	22.5	-22.5	0	22.5	60
2	45	22.5	0	-22.5	-45	0	45	22.5	0	-22.5	-45	-22.5	0	0	22.5	45	0	0	-45	-22.5	22.5	-22.5	0	22.5	0
3	22.5	0	-22.5	-45	-22.5	0	22.5	45	0	-45	0	45	0	0	22.5	45	0	0	-45	-22.5	22.5	-22.5	0	22.5	0
4	45	0	-45	0	45	0	-45	0	45	0	-45	0	45	0	-45	0	45	0	-45	0	-45	0	45	0	0
5	45	45	0	-45	-45	0	45	45	0	-45	-45	0	0	0	45	45	0	0	-45	-45	0	0	45	0	45
6	45	45	22.5	0	-22.5	-45	-45	-22.5	0	0	45	22.5	0	0	22.5	-22.5	-45	0	-22.5	0	22.5	-22.5	0	22.5	0

Table 1 – Investigated stackups to study the effect of changing ply orientation on the flutter stability

3. Theory and Methodology

Aeroelastic (flutter) stability of blade is influenced by a number of factors relating to structural dynamics, mechanical damping, airfoil and flow [7]. The airfoil and flow parameters are fixed by the operational requirements and the mechanical damping parameters are difficult to model due to complexities like contact phenomena. Thus the structural dynamics factors which include frequency and mode shapes, potentially remain the free variables to optimize and achieve flutter stability. Composites by definition are materials which are formed by stacking plies made of different materials like

fibers and matrix with each individual ply having a different orientation with a reference structural axis (1 2 3) as shown in Figure 3.

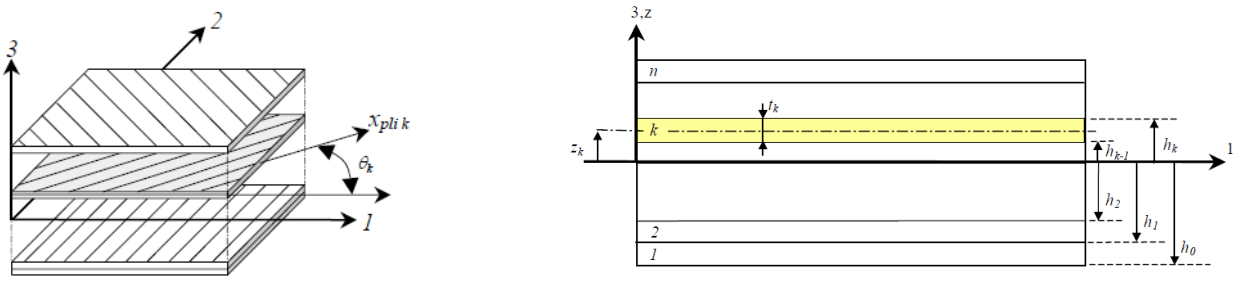

Figure 3 – A representative laminate [9]

The properties of the stacked plies (laminate) depend on properties of fibers and matrix forming the plies, their volume fractions and the thickness (t_k), position (h_k) and orientation (θ_k) of each ply with respect to symmetry axis. The stiffness matrix of the laminate is derived from the kinematics of Kirchoff's plate [11] which gives the relation of loads (N) and moments (M) to the strains (ε) and curvature (κ) through the stiffness matrix and is given in Equation 1

$$\begin{bmatrix} N_1 \\ N_2 \\ N_6 \\ M_1 \\ M_2 \\ M_6 \end{bmatrix} = \begin{bmatrix} A_{11} & A_{12} & A_{16} & B_{11} & B_{12} & B_{16} \\ A_{12} & A_{22} & A_{26} & B_{12} & B_{22} & B_{26} \\ A_{16} & A_{26} & A_{66} & B_{16} & B_{26} & B_{66} \\ B_{11} & B_{12} & B_{16} & D_{11} & D_{12} & D_{16} \\ B_{12} & B_{22} & B_{26} & D_{12} & D_{22} & D_{26} \\ B_{16} & B_{26} & B_{66} & D_{16} & D_{26} & D_{66} \end{bmatrix} \begin{bmatrix} \varepsilon_1^0 \\ \varepsilon_2^0 \\ \varepsilon_6^0 \\ \kappa_1^0 \\ \kappa_2^0 \\ \kappa_6^0 \end{bmatrix} \tag{1}$$

The terms A_{ij} denote the in-plane extensional stiffness terms while the terms D_{ij} denote the out-of plane bending stiffness terms. The terms B_{ij} represent the coupling between the in-plane and out-of plane stiffness terms. The relations for these terms are presented in Equation 2, 3, 4

$$A_{ij} = \sum_{k=1}^{n} [Q_{ij}(\theta_k)](h_k - h_{k-1}) \tag{2}$$

$$B_{ij} = \frac{1}{2} \sum_{k=1}^{n} [Q_{ij}(\theta_k)](h_k^2 - h_{k-1}^2) \tag{3}$$

$$D_{ij} = \frac{1}{3} \sum_{k=1}^{n} [Q_{ij}(\theta_k)](h_k^3 - h_{k-1}^3) \tag{4}$$

From these equations the orientation of fibers in a ply and the position of the ply present us free variables to tailor the stiffness of the laminate forming the blade thus influencing the structural dynamics factors to improve aeroelastic stability.

A parametric study is thus conducted to investigate the effect of change in ply orientation in laminate layups on the static and modal properties of the blade and finally the aeroelastic stability. For each stackup the composite layup in imported in Ansys Mechanical as a solid model and static and pre-stressed modal analysis accounting for pressure and centrifugal loads is performed. The mode shapes are extracted to impose in blade flutter analysis in Ansys CFX. The fourier transform time integration method is used with k-ε turbulence model. The aerodynamic damping work obtained from CFX for the first two modes (1st bending and 1st torsion) is used as a measure of aeroelastic stability. The damping work is determined from the work performed by the blade per cycle of vibration and is given by the relation in Equation 5 [8]. This work is given by the product of the pressure (p) and blade vibration velocity (v) in blade surface normal (n) direction integrated over the area of the blade and over time period of one oscillation. A positive value of work as computed by Ansys CFX indicates

a stable stackup while negative values indicate flutter instabilities. A comparison is made with the baseline metallic blade made of titanium alloy Ti-6Al-4V.

$$W_{Cycle} = \int_{t_0}^{t_0+T} \int_A p\vec{v}.\hat{n}\, dA dt \tag{5}$$

A damping factor (δ) and damping ratio (ξ) is also evaluated which is obtained by the normalization of aerodamping work using the relation in Equation 6 and 7 where s is the scaling factor used in Ansys to scale down modal amplitudes and ω is the blade vibration frequency [12].

$$\delta = \frac{W_{aero}}{4.K.E} = \frac{W_{aero}}{4.\frac{(s\omega)^2}{4}} \tag{6}$$

$$\xi = \frac{\delta}{2\pi} = \frac{W_{aero}}{2\pi(s\omega)^2} \tag{7}$$

4. Results

4.1 Mesh Independence

The solid mesh defining the composite model is generated from the surface mesh on the camber surface. Thus the camber surface mesh is refined to have 3 mesh cases and the modal frequencies are used as a variable to study convergence. A reference stackup with all plies oriented at 0° is used for the study. The meshes and corresponding results are represented in Table 2.

Case	No. of nodes	Mode 1 [Hz]	Mode 2 [Hz]	Mode 3 [Hz]	CPU time [min]
Coarse	105125	476.24	633.4	962.36	6.16
Medium	186918	478.37	638.03	962.39	8.44
Fine	404415	482.47	642.95	971.29	89.46

Table 2 – Modal frequency and CPU time from mesh independence study of composite model

From the results it is evident that all 3 mesh provide a converged results with a maximum variation of 1.5 % in the frequency values. The CPU time however is significantly higher for the fine mesh. The probable reason along with a higher mesh size is the hardware limitations on the system being used for simulations. As the time taken and results from the coarse and medium mesh are well within reasonable limits the medium mesh is opted for the simulations in the project.

Further referring to documentation in Ansys [8] it is suggested to use multiple elements per ply thickness to ensure accurate simulation. A check is thus performed to investigate the influence of multiple elements/ply on the results and the results are presented in Table 5.

Elements/ply	No. of nodes	Mode 1 [Hz]	Mode 2 [Hz]	Mode 3 [Hz]	CPU time [min]
1	186918	478.37	638.03	962.39	8.44
2	369054	478.39	638.08	962.35	100.16

Table 3 – Modal frequency and CPU time results for influence of multiple elements per ply thickness

The increase in number of elements/ply is observed to have negligible effect on the results and 1 element/ply is considered for current study. The study on the surface mesh size and the number of elements per ply thus provides a reliable model providing converged results.

Next taking a look at the distribution of ply drops in Figure 2 it is observed that few plies have a considerably shorter length. It is of interest to check the contribution of these plies to the overall vibration behaviour. This is done by assigning a 45° angle to shorter plies 13, 14, 19, 20, 21 and 22 while other angles are maintained at 0° angle same as the reference configuration. This stackup is referred as Stackupshort. A comparison of this stackup is made with reference stackup and the results are compared in Table 4

	Mode 1 [Hz]	**Mode 2 [Hz]**	**Mode 3 [Hz]**
Stackupshort	478.37	638.03	962.39
Reference stackup	480.01	626.33	962.42

Table 4 – Influence of selected shorter plies on the frequency values of the composite blade model

It can be seen that the mentioned short plies have a maximum of 1.8 % variation in the Mode 2 frequency and very negligible effect on the other two modes. Thus they majorly serve the purpose of adjusting the overall composite structure to the blade shape. Hence while changing the ply angles and deciding the stackup the focus is kept on the stacking sequence of the longer plies on the outer surface of the stackup.

4.2 Static analysis results

The maximum static deflection is observed to occur near the leading edge tip region. The maximum static displacement is observed for Stackup 5 which has a higher number of $\pm 45^\circ$ plies in the stackup and 45° ply on the outer surface. The minimum is observed for Stackup 3 which has higher number of $\pm 22.5^\circ$ plies in stackup and 22.5° ply on the outer surface. Stackup 4 having a higher number of 0° plies in the stackup and 45° ply on the outer surface shows the second lowest static displacement. Thus lower value of ply angles in the stackup and their placement on outer surface is seen to result in lower static displacement value. The maximum value of static displacement observed across all stackups is 0.74 mm which is lower than maximum displacement of the titanium Ti-6Al-4V blade which was 1.3 mm.

Stackup	**1**	**2**	**3**	**4**	**5**	**6**
Deflection [mm]	0.69	0.64	0.59	0.62	0.74	0.70

Table 5 – Maximum static deflection for the six investigated stackups

4.3 Modal analysis results

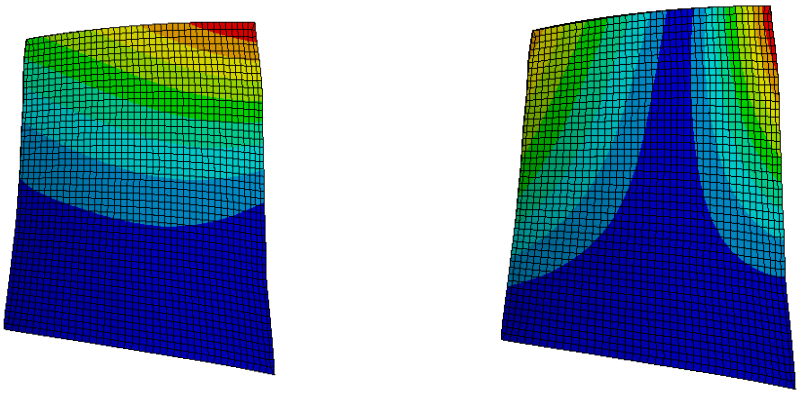

(a) Mode 1

(b) Mode 2

Figure 4 – First two modes obtained from the modal analysis

The modal analysis provides the modal frequencies and mode shapes of which the first two modes are of interest and presented in Figure 4. It is observed that the 1^{st} mode exhibits a bending like behaviour with a twisting portion and 2^{nd} mode a torsion like behaviour. It is of further interest to understand the effect of the ply angle configuration on the mode shape and frequencies. Thus a relation between the stackup stiffness terms with the twisting at the blade tip and modal frequency is investigated. The twisting is calculated from the blade tip edge to edge deflection of mode. The stiffness here is calculated according to classical laminate theory for an equivalent laminate with no ply drops as represented in Figure 3 and having the ply stackup configuration as of the investigated stackups. The stiffness values do not represent the actual stiffness values of the blade but represent a

stiffness value of one equivalent mesh element encompassing the investigated stackup configuration. The term A_{11} is the longitudinal stiffness term while the term A_{66} is the shear stiffness term of inplane stiffness while D_{11} is the bending and D_{66} torsion stiffness terms of the out of plane terms.

4.3.1 Mode 1

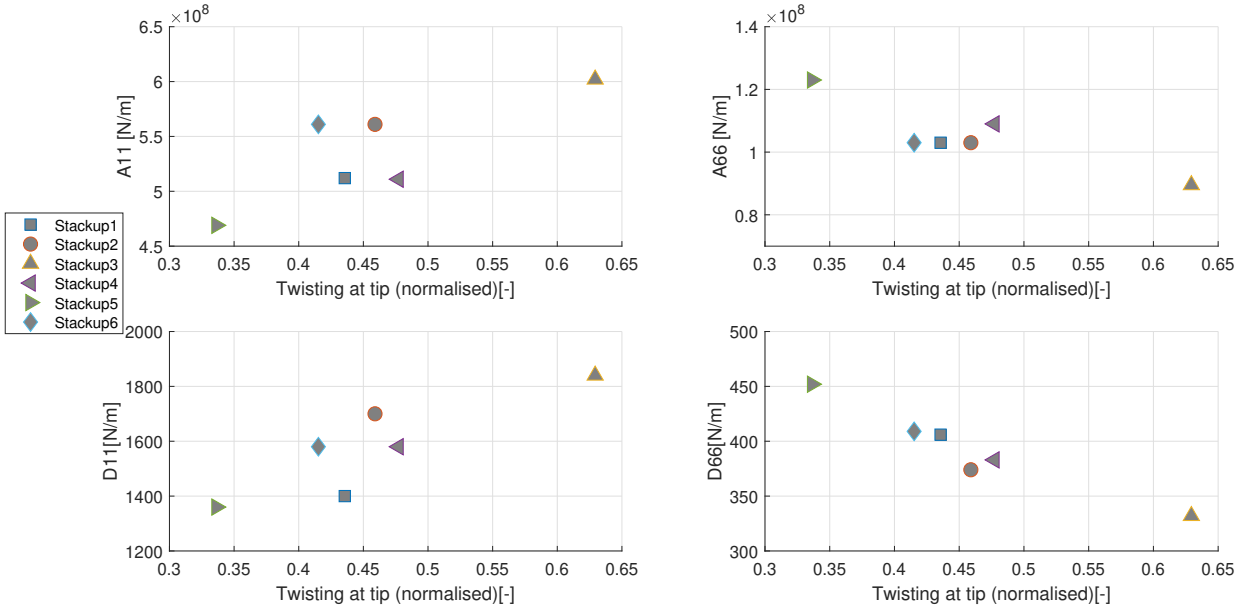

Figure 5 – Stiffness terms A11, A66, D11 and D66 plotted against the twisting at tip for mode 1

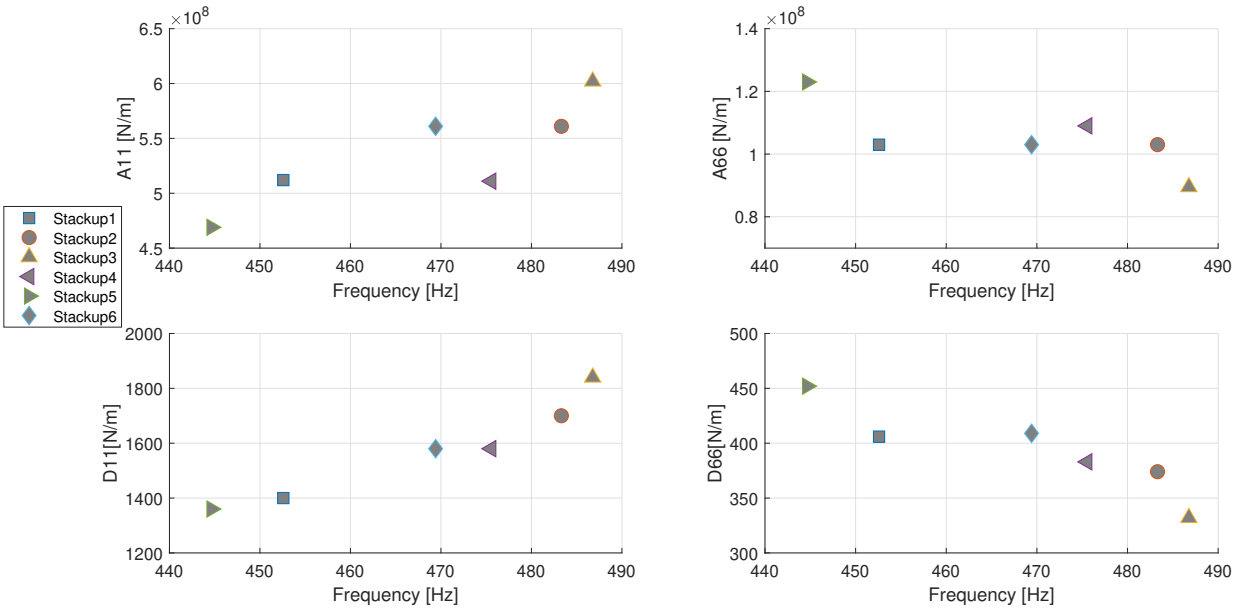

Figure 6 – Stiffness terms A11, A66, D11 and D66 plotted against the modal frequency for mode 1

Stackup 5 $[(45/45/0/\text{-}45/\text{-}45/0)_2/...]_s$ has higher number of $\pm 45^\circ$ plies and placed towards exterior of the stackup thus exhibiting a higher torsional (D_{66}) stiffness leading to lower twisting. This in turn results in lower number of 0° plies in the stackup thus a lower bending (D_{11}) stiffness leading to lower bending frequency. Similarly Stackup 3 $[22.5/0/\text{-}22.5/\text{-}45/\text{-}22.5/0/22.5/45/0/\text{-}45/0/45/...]_s$ having higher number of $\pm 22.5^\circ$ plies exhibits a higher D_{11} stiffness driving up the bending mode frequency and a lower D_{66} stiffness leading to a higher twist at the blade tip. Comparing Stackup 2

[(45/22.5/0/-22.5/-45)/0/(45/22.5/0/-22.5/-45)/-22.5/...]$_s$ and Stackup 6 [(45/45/22.5/0/-22.5/-45/-45)/-22.5/0/0/45/22.5/0/...]$_s$ both have the equal number of plies for each angle thus having the same value for A_{11} and A_{66} terms. However Stackup 6 has more 45° plies placed towards the outside of the stackup thus having higher D_{66} stiffness and a lower twisting and lower D_{11} stiffness and lower bending frequency. Thus having higher number of ±45° plies and their placement towards outer surface of stackup will lead to lower twisting while having higher 0° plies and placed outwards will lead to higher bending mode frequency. A compromise between lower twisting and higher frequency can be achieved by evenly placing lower angle plies between ±45° plies as in Stackup 2 and Stackup 6.

4.3.2 Mode 2

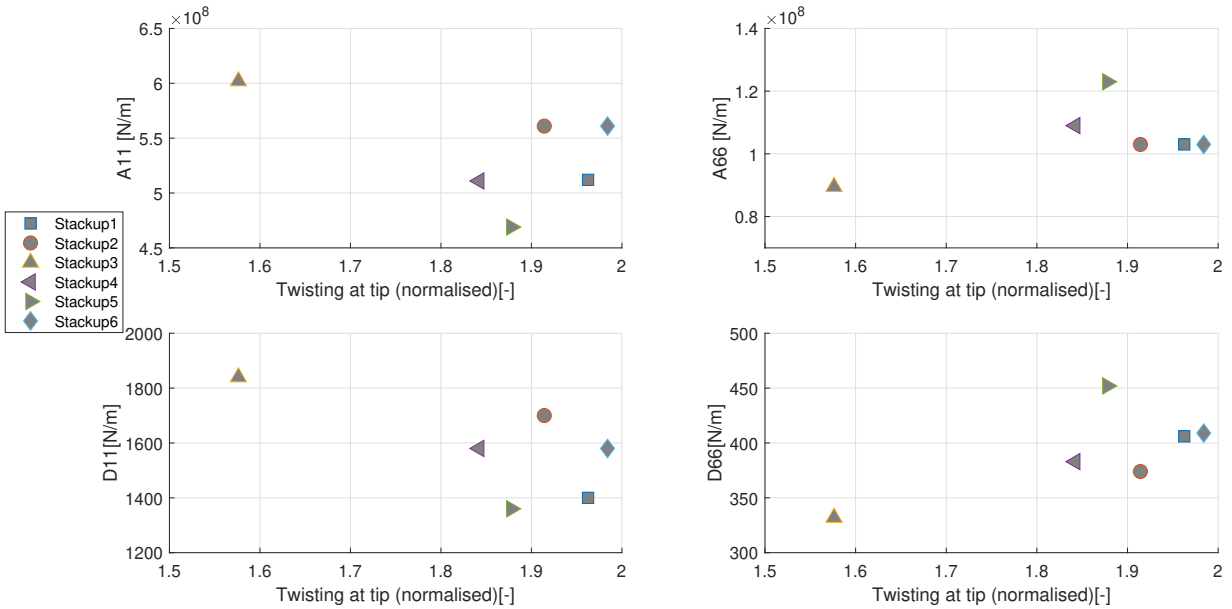

Figure 7 – Stiffness terms A11, A66, D11 and D66 plotted against the twisting at tip for mode 2

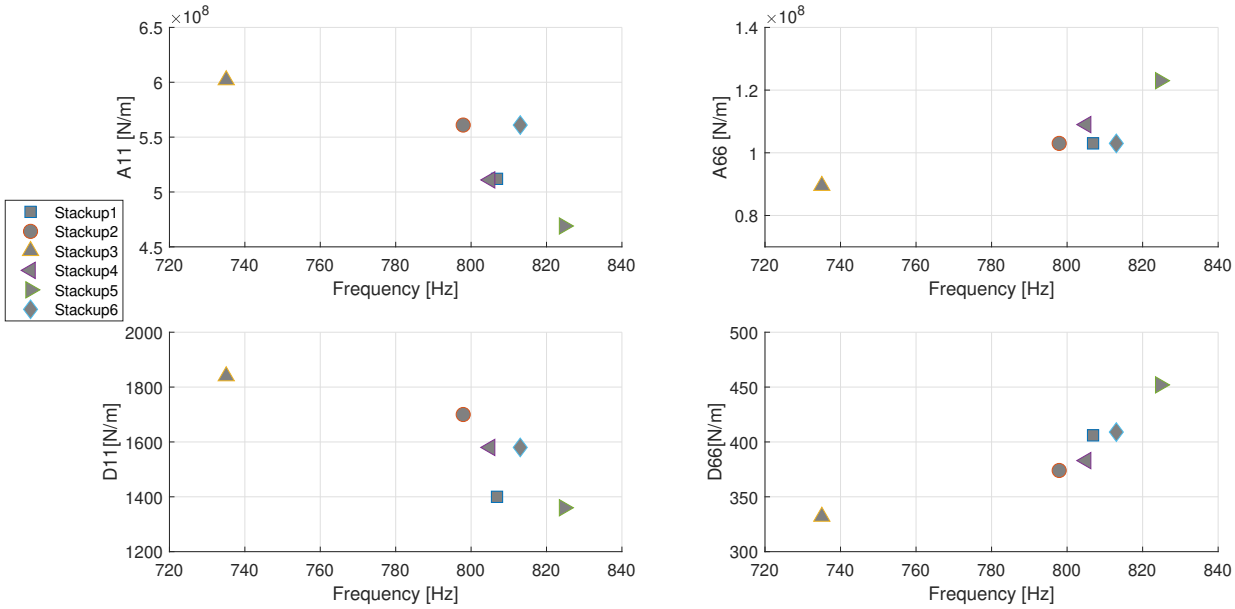

Figure 8 – Stiffness terms A11, A66, D11 and D66 plotted against the modal frequency for mode 2

Stackup 3 with lower angles and thus lowest torsional (D_{66}) stiffness exhibits the lowest Mode 2 (torsion) frequency and Stackup 5 with $\pm 45^{\circ}$ plies has highest D_{66} stiffness and thus highest Mode 2 frequency. The twisting however is observed to be lowest in Stackup 3 and an intemediate value for Stackup 5. Stackup 3 having the lowest twisting has higher $\pm 22.5^{\circ}$ and 0° plies and Stackup 4 with the second lowest twisting has higher number of 0° plies. A strong correlation of ply angles with the twisting at tip in the mode shape is not established for other stackups. The only observation made is stackups with more lower angles and placed on the exterior exhibit lower twisting. This is further elaborated with the aerodamping results by looking at the shape of the twisted tip for each stackup and their comparison to conventional torsion behaviour.

4.4 Aerodynamic damping

4.4.1 Mode 1

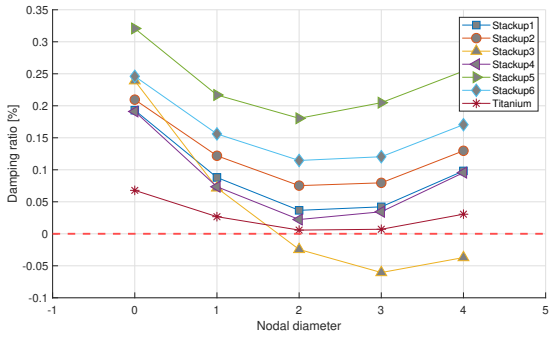

(a) Aerodynamic damping ratio vs nodal diameter

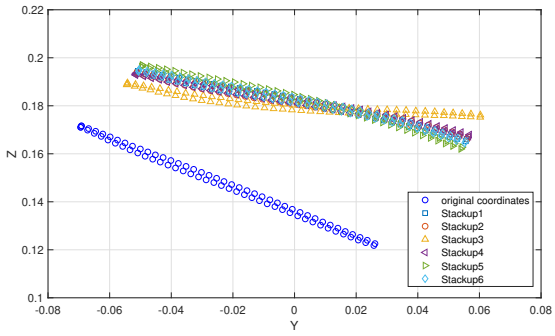

(b) Mode shape at the tip of blade

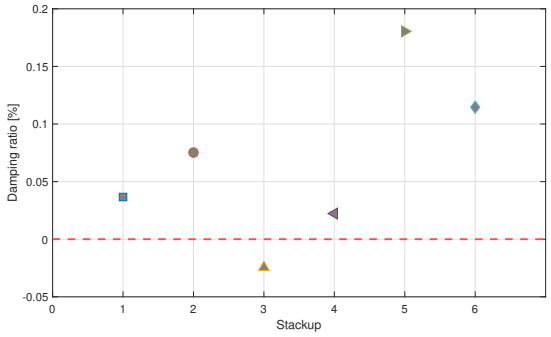

(c) Aerodamping for the least stable nodal diameter

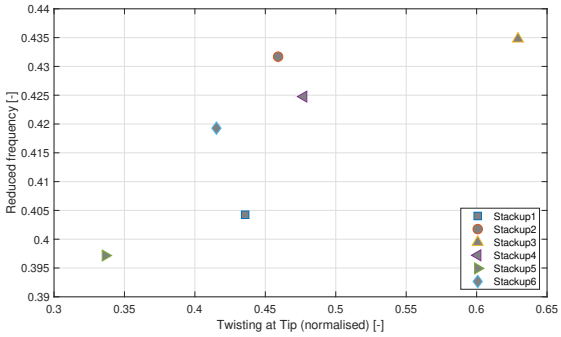

(d) Reduced frequency vs twisting at blade tip

Figure 9 – Aerodamping work compared with reduced frequency and twisting in mode shape for mode 1

As mentioned in theory the frequency and mode shape are decisive to flutter stability. Figure 9a presents the damping ratio for a number of Nodal diameters (ND), Figure 9c is additional plot representing damping only at least stable ND for each stackup, the mode shape at the blade tip is plotted in Figure 9b and the reduced frequency and twisting at blade tip is presented in Figure 9d. Due to high computational effort a limited number of Nodal diameters (ND) are analysed while ensuring a local minimum of damping ratio is observed within the investigted NDs. The frequency is represented as the non dimensional reduced frequency and is calculated using the relation 8 [2], where reduced frequency (k) is the multiple of blade vibration frequency (f) in [Hz] and reference length (L_{ref}) divided by the reference flow velocity (U_{ref}). The L_{ref} is half chord length and the U_{ref} is the mass flow averaged velocity at the domain inlet.

$$K = \frac{2\pi f L_{ref}}{U_{ref}} \tag{8}$$

Stackup 3 is the least stable stackup with negative damping for ND 2 and 3 with lowest at ND 3. All other stackups and the titanium blade show the least stability at ND 2. Stackup 3 with negative damping shows the highest twisting at the tip and highest reduced frequency while the most stable Stackup 5 has the lowest twisting and the lowest reduced frequency. The twisting value is seen to dominate in these comparison where the higher twisting leads the Stackup 3 into unstable behaviour. The higher twisting in Stackup 3 $[22.5/0/\text{-}22.5/\text{-}45/\text{-}22.5/0/22.5/45/0/\text{-}45/0/45/...]_s$ is an effect of the lower torsion stiffness due to lower value of ply angles on the stackup exterior. Similarly Stackup 5 $[(45/45/0/\text{-}45/\text{-}45/0)_2/...]_s$ shows lower twisting due to higher torsion stiffness provided by $\pm 45^\circ$ plies. Considering Stackup 6 and Stackup 1 or Stackup 2 and Stackup 4 in which the amount of twisting is relatively close the stackup with higher reduced frequency is observed to have a higher aerodamping ratio. This higher reduced frequency in Stackup 2 and Stackup 6 is due to the higher number of lower angles compared to Stackup 4 and stackup 1 respectively. Comparing Stackup 1 and Stackup 2, it is observed that Stackup 2 has a higher twisting and a significantly higher reduced frequency. Here the higher reduced frequency dominates thus exhibiting a higher aerodamping ratio for Stackup 2. Between Stackup 2 $[(45/22.5/0/\text{-}22.5/\text{-}45)/0/(45/22.5/0/\text{-}22.5/\text{-}45)/\text{-}22.5/...]_s$ and Stackup 6 $[(45/45/22.5/0/\text{-}22.5/\text{-}45/\text{-}45)/0/(..)/\text{-}22.5/...]_s$ having equal number of each ply angles the twisting in Stackup 6 is lower due to higher $\pm 45^\circ$ plies on the exterior which dominates and leads to more stability. Thus it can be concluded that for Mode 1 (bending) a combination of twisting and reduced frequency plays a role in the stability of the stackup. A balanced combination of lower twisting achieved by having $\pm 45^\circ$ plies and higher reduced frequency achieved using lower angles is desired for stability. For stackups with relatively similar amount of twisting the stackup with higher reduced frequency will tend to more stability. It is recommended to avoid lower angles on stackup exterior to prevent instabilities and have them sandwiched between $\pm 45^\circ$ plies placed on the stackup exterior to minimize twisting and maximise bending mode frequency as in Stackup 2 and 6.

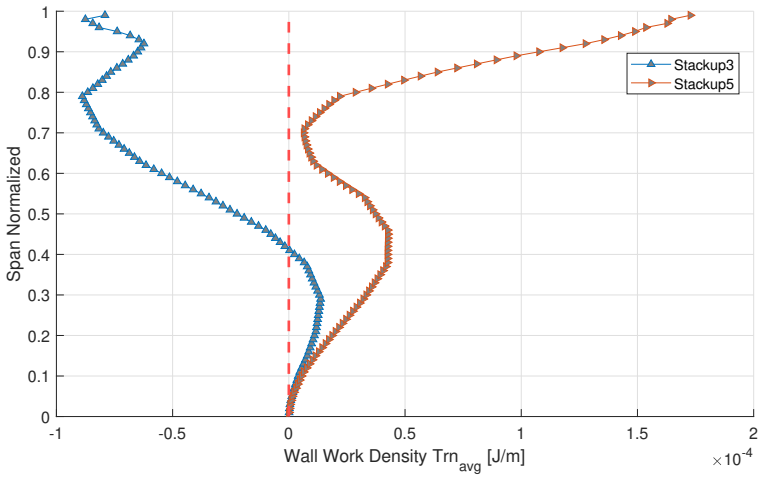

Figure 10 – Spanwise wall work density distribution over the blade for mode 1

The wall work density distribution along the span is looked at for the most stable Stackup 5 and unstable Stackup 3 in Figure 10. It can be observed that Stackup 3 shows a negative work density on most span of the blade with a positive work only on 40 % span of blade from the hub. The negative values increase considerably beyond 50 % span. Stackup 5 has a positive work density on the complete span. The region above 80% span to the tip is seen to have a bigger contribution towards stability of Stackup 5. This reaffirms the significance of mode shape tailoring at the tip to minimize twisting for flutter stability.

4.4.2 Mode 2

From Figure 11a it is observed for Mode 2 all the stackups exhibit a stable behaviour and a damping ratio higher than the titanium blade. All composite stackups, except for Stackup 3, show a minimum value of work and damping ratio for nodal diameter 5 or 6. Stackup 3 shows a minimum value for

nodal diameter 11 and the curve of work and damping ratio can be observed to have a shift compared to other stackups. To investigate this effect, the mode shape of the blade are observed at the tip as shown in Figure 11b. Qualitatively observing the deflection of tip, it is observed that Stackup 3 has the inflection point moved towards the leading edge (right) of the blade. Also the trailing edge (left) of the blade is less deflected and the mode shape is seen to bulge after the inflection point towards the trailing edge thus deviating the mode shape from conventional torsional behaviour. This can be seen as a result of having 22.5° plies on the outer surface of the stackup. This leads to lower twisting of the blade.

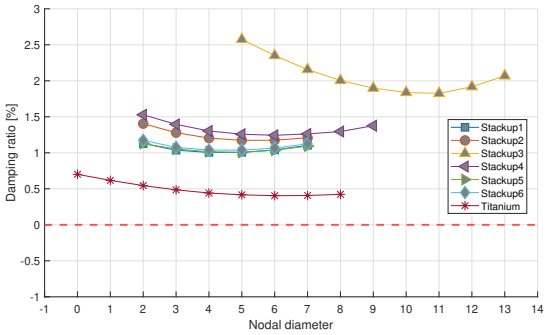

(a) Aerodynamic damping ratio vs nodal diameter

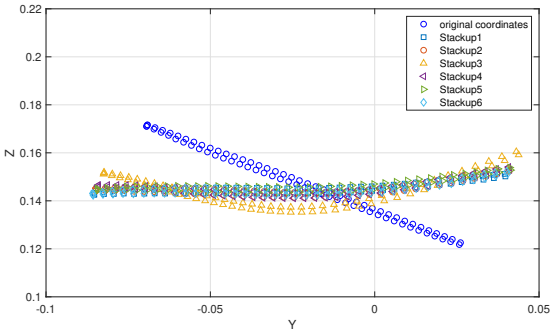

(b) Mode shape at the tip of blade

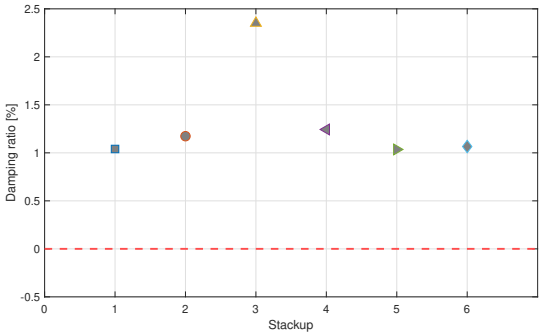

(c) Aerodamping for the least stable nodal diameter

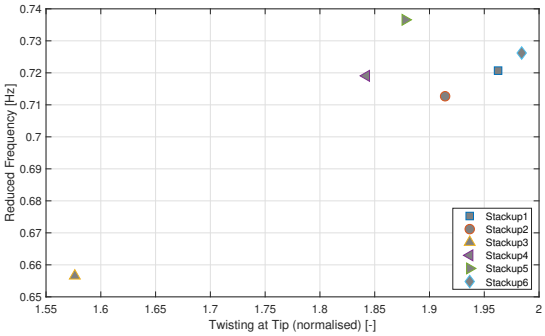

(d) Reduced frequency vs twisting at blade tip

Figure 11 – Aerodamping work compared with reduced frequency and twisting in mode shape for mode 2

From Figure 11d and 11c, Stackup 3 having 22.5° plies on the outer surface has the highest damping ratio and lowest twisting which is an effect of an unconventional torsion mode shape. This is followed by Stackup 4 which has relatively higher number of 0° towards the outer surface and shows the second highest value for damping ratio and second lowest value for twisting. Stackup 5 with higher number of $\pm 45°$ plies towards the outer surface exhibits the lowest damping ratio and has a intermediate value of twisting and highest value of reduced frequency. The damping ratio values for stackups other than Stackup 3 are quite close and strong relation between reduced frequency and twisting cannot be stated here. It can only be concluded that using lower value of ply angle towards the outer plies in the stackup lead to stable behaviour in Mode 2.

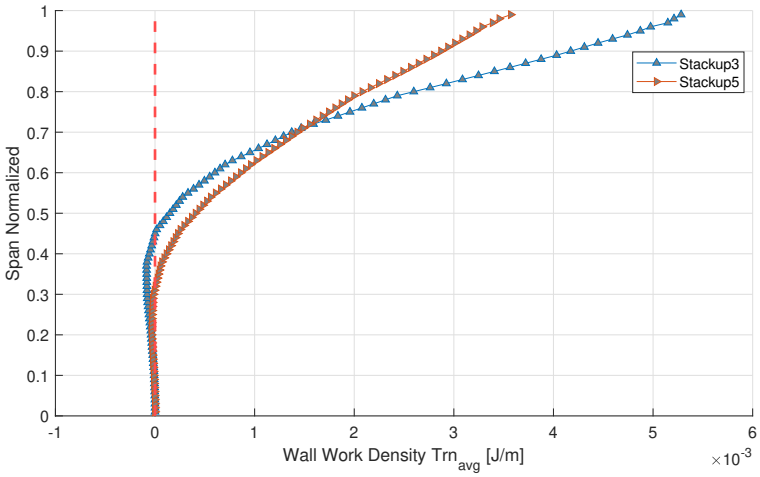

Figure 12 – Spanwise wall work density distribution over the blade for mode 2

Looking at the Wall work density distribution along the span in Figure 12 both the Stackup 5 and Stackup 3 show similar positive wall work density distribution along span. Deviations are only observed from 70 % span towards the tip, where the Stackup 3 exhibits more stabilizing distribution of the wall work density.

5. Conclusion

The objectives to design a composite blade in Ansys ACP, and establish the relation between ply angle configurations in stackup and aeroelastic stability were achieved. The anisotropic properties of composites are found to have a potential in tailoring the vibration behaviour by changing the angles and their distribution in the ply stackup and have a stabilising or destabilising effect on the flutter behaviour. A methodology to build the composite model was established which once created gave a easy approach to modification of stackup angles and ply lengths using the built-in excel interface.

Six different ply stackup configurations were investigated in the scope of project with a combinations of $\pm 60^\circ$, $\pm 45^\circ$, $\pm 22.5^\circ$ and 0° plies. The modal analysis results for Mode 1, indicated a decrease in shear and torsional stiffness and a higher twisting in the mode shape for a stackup with higher number of $\pm 22.55^\circ$ and 0° plies and arrangement of those plies on outer surface. The lowest twisting was exhibited by stackups with higher number of $\pm 45^\circ$ and their arrangement on outer surface. These stackups with lower twisting due to $\pm 45^\circ$ plies exhibited higher stability in flutter. For stackups with same number of plies of particular angle the twisting and stiffness showed a dependency on the the arrangement of plies. For similar twisting stackups with higher frequency were more stable. The only unstable stackup was with higher number of $\pm 22.5^\circ$ towards the outer surface and the highest twisting. Overall a lower twisting at the tip and higher reduced frequency was found favourable for flutter stability in Mode 1.

For Mode 2, stackups with higher number of $\pm 45^\circ$ resulted in higher torsional stiffness and higher frequencies. In terms of twisting a contradictory effect was observed with respect to Mode 1, as the plies with lower angles and thus lower torsional stiffness were found to deviate the mode shape from conventional torsion behaviour and reduce the twisting at the tip. This led to the least stable stackup for Mode 1 with 22.5° ply towards the outer surface to have the highest stability for Mode 2 and the most stable stackup in Mode 1 with $\pm 45^\circ$ plies to have least stability in Mode 2 . Thus a stackup with stabilising behaviour in one mode could have a destabilising effect for the other mode.

The dependency on ply angle and arrangement of plies is observed to be complex and further investigation of other ply angles (like $\pm 15^\circ$ and $\pm 30^\circ$) and experimental validation is therefore deemed necessary.

6. Future work

Further implementation of the approach presented here is currently carried out within the framework of the EleFanT (Electric Fan Thrusters) project funded by the Swedish Energy Agency through "Fossilfritt flyg 2045" program. The aeroelastic tailoring is being applied in the design of the carbon fiber composite fan blades developed in the project. The prototypes of the composite fan blade will be manufactured and blade vibrational behaviour will be assessed experimentally, providing necessary validation data for the model.

7. Contact Author Email Address

Contact author email address mailto: chalke@kth.se

8. Copyright Statement

The authors confirm that they, and/or their company or organization, hold copyright on all of the original material included in this paper. The authors also confirm that they have obtained permission, from the copyright holder of any third party material included in this paper, to publish it as part of their paper. The authors confirm that they give permission, or have obtained permission from the copyright holder of this paper, for the publication and distribution of this paper as part of the ICAS proceedings or as individual off-prints from the proceedings.

References

[1] Bendiksen O.O. Recent developments in flutter suppression techniques for turbomachinery rotors. *Journal of Propulsion*. Vol. 14 No. 2, pp 164-171, 1987.

[2] Reiber C, Blocher M. Potential of aeroelastic tailoring to improve flutter stability of turbomachinery compressor blades. *Proceedings of 12th ETC conference*, Stockholm, ETC2017-180, 2017.

[3] Lejon M, Grönstedt T, Glodic N, Petrie-Repar P, Genrup M Mann A. Multidisciplinary design of a three stage high speed booster. *Proceedings of ASME Turbo Expo Conference*, Charlotte, GT2017-64466, 2017

[4] Jiaguangyi Xiao, Yong Chen, Qichen Zhu, Jun Lee, Tingting Ma. A general ply design for aeroengine composite fan blade. *Proceedings of ASME Turbo Expo 2017: Turbomachinery Technical Conference and Exposition*, Charlotte, GT2017-64377, 2017.

[5] Irisarri F. X, Lasseigne A, Leroy F.H, Le Riche R. Optimal design of laminated composite structures with ply drops using stacking sequence tables. *Composite Structures*, Vol:107, January 2014, Pages 559-569, 2014.

[6] Carta F.O. Coupled blade-disk-shroud flutter instabilities in turbojet engine rotors. *Journal of Engineering for Power*, Pages 419 – 426, 1967.

[7] Montgomery M,Tartibi M, Eulitz F, Schmitt S Application of unsteady aerodynamics and aeroelasticity in heavy duty gas turbines. *ASME Turbo Expo 2005: Power for Land, Sea, and Air. American Society of Mechanical Engineers*, pp. 635–649, 2005.

[8] Ansys. Ansys users guide. *Ansys Help Documentation R3*, 2019.

[9] Michaël Bruyneel. A course on mechanics of composites *University of Liege*, 2020-2021.

[10] Aeromechanics course notes *KTH, Stockholm*, 2019-2020.

[11] Jones Robert M. Mechanics Of composite materials, Second edition. Taylor and Francis, Inc., 1999.

[12] Stasolla V. Numerical analysis of aerodynamic damping in a transonic compressor. *Master Thesis, KTH School of Industrial engineering and Management*, 2019.